Hindawi Publishing Corporation
International Journal of Photoenergy
Volume 2014, Article ID 854749, 6 pages
http://dx.doi.org/10.1155/2014/854749

Research Article

Enhancing the Efficiency of Polymer Solar Cells by Modifying Buffer Layer with N,N-Dimethylacetamide

Shaopeng Yang, Xuefeng Sun, Ye Zhang, Guang Li, Xiaohui Zhao, Xiaowei Li, and Guangsheng Fu

Hebei Key Laboratory of Optic-Electronic Information Materials, College of Physics Science and Technology, Hebei University, Baoding, Hebei 071002, China

Correspondence should be addressed to Shaopeng Yang; spyang@hbu.edu.cn and Guangsheng Fu; fugs@hbu.edu.cn

Received 27 June 2014; Revised 3 October 2014; Accepted 4 October 2014; Published 20 October 2014

Academic Editor: Niyaz Mohammad Mahmoodi

We modified the PEDOT:PSS anode buffer layer in P3HT:PCBM bulk heterojunction polymer solar cells by spin-coating the solvent N,N-dimethylacetamide (DMAC). This modification significantly enhanced the efficiency of the ITO/PEDOT:PSS/DMAC/P3HT:PCBM/LiF/Al solar cells. The DMAC-treated device spin-coated at 3000 rpm exhibited a power conversion efficiency (PCE) of 3.74%, a 59% improvement over that of an untreated cell. To study the mechanism of improving the conversion efficiency, we characterized many parameters, including the light and dark *I-V* curves, external quantum efficiency, active layer absorption spectrum, transmission spectrum of ITO:PEDOTPSS, PEDOT:PSS surface morphology, and electrical conductivity. Modifying the PEDOT:PSS film increased conductivity, making it more conducive to hole extraction and collection. Our findings suggest that modifying the anode buffer layer can improve photoelectric conversion efficiency.

1. Introduction

Solar energy is sustainable and clean, making it increasingly important in global power production [1–8]. Organic photovoltaics attract much interest because they are inexpensive, nontoxic, easy to prepare, and easy to build into flexible devices. One way to improve the performance of organic photovoltaics is using a blended bulk heterojunction. This structure increases the contact area between the electrode and electron acceptor, increasing the carrier diffusion and transmission and reducing recombination of excitons. However, the conversion efficiency of a cell is greatly affected by the energy level between its electrode and electron donor (acceptor). The structure and properties of these interfaces determine the transmission and diffusion of charge. In theory, a good ohmic contact not only improves charge collection but also can promote charge diffusion and reduce charge recombination, thereby improving conversion efficiency [9–11].

To optimize the interfacial properties between the donor (acceptor) and the electrode, a buffer layer can be introduced. This layer can reduce leakage current, increasing the open-circuit voltage and fill factor while improving device stability [12, 13]. Anode buffer layers, which have been researched thoroughly, are mainly composed of a metal oxide, such as molybdenum trioxide (MoO_3), or a conducting polymer such as PEDOT:PSS. However, few studies have investigated modifying the buffer layer. Jung et al. prepared an ITO/MoO_3/P3HT:PCBM/LiF/Al organic solar cell, using 10 nm of MoO_3 as the anode buffer layer. This cell exhibited a power conversion efficiency (PCE) as high as 4.2%, showing that including a buffer layer can improve the performance of organic solar cells (OSCs). Jung et al. [14] studied OSCs with buffer layers made from MoO_3 and PEDOT:PSS. The MoO_3 buffer layer was superior to PEDOT:PSS in reducing leakage current, increasing device parallel resistance, and increasing open-circuit voltage. Subbiah et al. [15] prepared an ITO/PEDOT:PSS/CuPc/C60/BCP/Al cell with a plasma-processed PEDOTP:PSS layer, finding that plasma processing the PEDOTP:PSS increased the fill factor (FF) from 0.36 to 0.41–0.49. Although the PEDOT:PSS thin film exhibited excellent performance, it had many defects. Thus, the anode performance must still be improved.

Many methods have been developed to improve PEDOT:PSS thin films, such as mixing with other

materials or adding dopants to the PEDOT:PSS suspension such as propylene glycol, sorbitol, or methyl sulfoxide. Adding substances with high boiling points can improve the conductivity of PEDOT:PSS by 2-3 orders of magnitude [16, 17]. Using a double buffer layer of MoO_3/TFB{poly(9,9-dioctylfluorene-co-N-[4-(3-methylpropyl)]-diphenylamine)} for the anode can also enhance hole collection and electron blockage, improving short-circuit current density (J_{sc}) and fill factor (FF). These devices have PCEs higher than those with PEDOT:PSS or MoO_3 buffer layers and have much higher stability.

In this paper, we enhance the performance of organic solar cells by modifying the anode buffer layer to improve hole delivery efficiency. To accomplish this, we doped and modified PEDOT:PSS with DMAC organic solvent [18].

2. Experiment

2.1. Materials and Reagents. In these experiments, we used commercial materials without further modification. The P3HT and PCBM (Luminescence Technology Corp.), PEDOT:PSS (Clevios PVP. AI 4083), and other chemicals were analyzed as pure.

PEDOT:PSS is a conductive blend of PEDOT [poly(3,4-thiophene monomer ethylene 2 oxygen)] and PSS (polystyrene sulfonate). DMAC (dimethylacetamide) is an aprotic polar solvent and has a high boiling point, good thermal stability, and good chemical stability. The most widely researched type of this polymer solar cell is the bulk heterojunction cell, which uses poly(3-hexylthiophene-2,5-diyl) (P3HT) and [6, 6]phenyl-C61-butyric acid methyl ester (PCBM) as electron donor and electron acceptor, respectively. These materials are conducive to research because they are more stable than similar donors and acceptors. PEDOT:PSS is widely used as an anode buffer layer in polymer batteries because it is highly transparent and environmentally friendly. It also has high charge transport capacity and can be prepared in solution and spin-coating [19].

2.2. Preparation of Solar Cells. In the present experiments, we used 3 × 4 cm glass substrates coated with ITO. The square resistance was 10 Ω/cm^2. After sealing parts of the substrates with tape, the remainder was etched with concentrated hydrochloric acid for 20 min and then cleaned with detergent to remove hydrochloric acid residue and impurities on the ITO. The samples were then ultrasonically cleaned for 10 min in deionized water, acetone, ethanol, and isopropanol sequentially. They were then dried on sheet glass with N_2 and then treated with UV-O_3 for 10 min to remove organic contamination on the ITO and to improve the ITO work function, improving hole transmission and collection. We performed five groups of experiments. First, PEDOT:PSS was spin-coated (KW-4) on ITO at 3000 rpm to a final film thickness of 30–35 nm, measured by a profilometer (Dektak 150, Veeco); this is denoted as sample A. Then, PEDOT:PSS and DMAC were mixed in a ratio of 4 : 1 (v/v) and spun at 3000 rpm; this is denoted as sample B. Then, DMAC was spin-coated onto PEDOT:PSS buffer layers at 1000, 3000, or 5000 rpm; these are denoted as samples C, D, and E, respectively. The five groups of samples were then annealed at 130°C for 10 min.

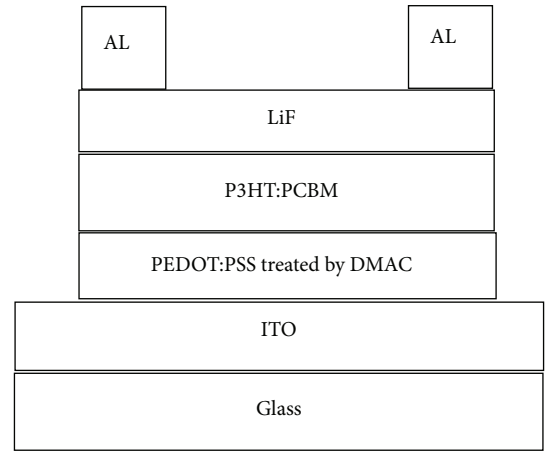

Figure 1: The device structure of the solar cells, P3HT:PCBM as the active layer and the PEDOT:PSS modified by the DMAC.

The P3HT:PCBM active layer (~100 nm thick) was fabricated by spin-coating a P3HT:PCBM solution (1 : 1 w : w; dissolved in chlorobenzene and chloroform, v : v 3 : 1) on the buffer layer. The device was then transferred into a vacuum chamber at 10^5 Torr. In this chamber, a LiF buffer layer (~1 nm thick) and an Al electrode (100 nm thick) were evaporated on the P3HT:PCBM active layer through a shadow mask. This process defined an active device area of 0.4 cm × 0.4 cm. The devices were then annealed at 130°C for 10 min. Figure 1 shows the final device structure.

2.3. Device Performance Test. The *J-V* response of each device (*J-V* curve) was stimulated by a sun simulator (AM1.5, 100 mW/cm^2; XES-200, Solar Simulator) and measured using a digital source meter (Keithley 2400). The illumination intensity of the solar simulator was calibrated using a standard cell (SRC-1000-TC-K-QZ, VLSI STANDARDS). These measurements were done at room temperature, using ITO as the anode and Al as the cathode. The light was irradiated from the ITO side of the device. The thickness of each layer was measured by a profilometer (Dektak 150, Veeco). Atomic force microscopy (AFM; di-Innova, Veeco) images were obtained in contact mode.

3. Results and Discussion

Table 1 shows the performance parameters for the five sets of cells. The device with the highest efficiency had DMAC spin-coated on the PEDOT:PSS layer at 3000 rpm. This device exhibited efficiency as high as 3.74%, short-circuit current density of 11.74 mA/cm^2, open-circuit voltage of 0.58 V, and fill factor of 0.55. Modifying the anode with DMAC did not change the open-circuit voltage. In bulk heterojunction polymer solar cells, the open-circuit voltage depends on the ohmic contact between active layer and the electrode, as well as the difference in energy levels between the highest level of

Table 1: The performance parameters of solar cell based on P3HT:PCBM with different volume ratios of nitrobenzene added in blend solutions.

Devices	PEDOT:PSS thickness (nm)	J_{sc}/(mA/cm^2)	V_{oc}/V	FF/%	R_s/(Ω·cm^2)	R_{sh}/(Ω·cm^2)	$\bar{\eta}$/%
A	35 ± 1	7.82	0.58	0.52	14.1	328	2.35%
B	32 ± 1	8.52	0.58	0.55	11.2	406	2.63%
C	30 ± 1	9.39	0.58	0.56	10.8	453	3.03%
D	30 ± 1	11.74	0.58	0.55	9.6	496	3.74%
E	31 ± 1	11.18	0.58	0.55	9.8	522	3.55%

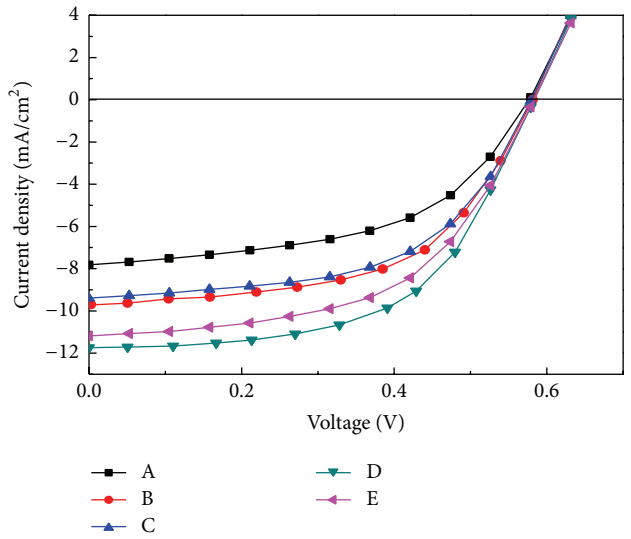

Figure 2: J-V curves of five different polymer solar cells. A: only PEDOT:PSS solution on ITO at the speed of 3000 rpm. B: the PEDOT:PSS and DMAC mixed in a ratio of 4 : 1 (v/v) at the speed of 3000 rpm. C, D, and E: the PEDOT:PSS buffer layer modified by DMAC at speed of 1000, 3000, and 5000 rpm.

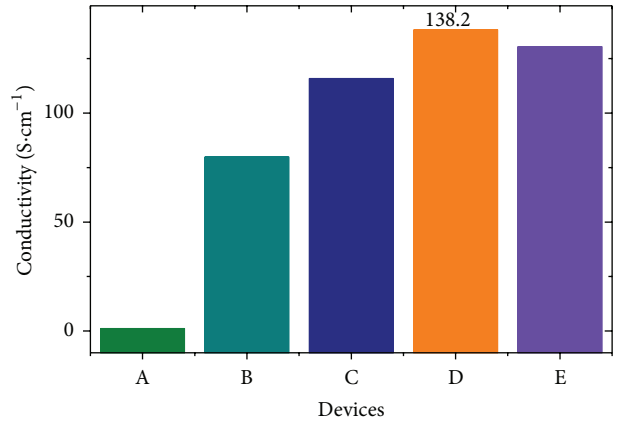

Figure 3: The conductivity of PEDOT:PSS corresponding to different devices (A: only PEDOT:PSS solution on ITO at the speed of 3000 rpm. B: the PEDOT:PSS and DMAC mixed in a ratio of 4 : 1 (v/v) at the speed of 3000 rpm. C, D, and E: the PEDOT:PSS buffer layer modified by DMAC at speed of 1000, 3000, and 5000 rpm).

the occupied electronic donor orbital and the highest level of the occupied electron acceptor orbital [20]. The PEDOT:PSS treated by DMAC had almost no effect on open-circuit voltage.

3.1. Analysis of I-V Characteristics. Inserting a PEDOT:PSS layer treated with DMAC substantially improved device performance, as shown in Figure 2. Compared with untreated devices, DMAC-treated devices had unchanged fill factor and open-circuit voltage, increased short-circuit current density from 7.82 mA/cm^2 to 11.74 mA/cm^2, and increased PCE from 2.35% to 3.74%. Combined with measurements of conductivity (Figure 3), these results show that using DMAC-treated PEDOT:PSS reduced the series resistance of the device.

3.2. Analysis of Conductivity. Figures 3 and 4 show the dark conductivity and J-V behavior of various devices. Among the devices treated with DMAC, sample D had much higher conductivity than samples A, B, C, and E. Increasing the film

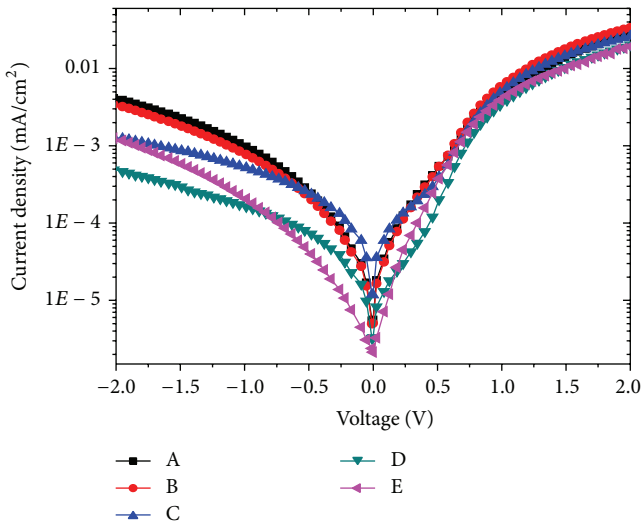

Figure 4: J-V curve of device under dark condition. A: only PEDOT:PSS solution on ITO at the speed of 3000 rpm. B: the PEDOT:PSS and DMAC mixed in a ratio of 4 : 1 (v/v) at the speed of 3000 rpm. C, D, and E: the PEDOT:PSS buffer layer modified by DMAC at speed of 1000, 3000, and 5000 rpm.

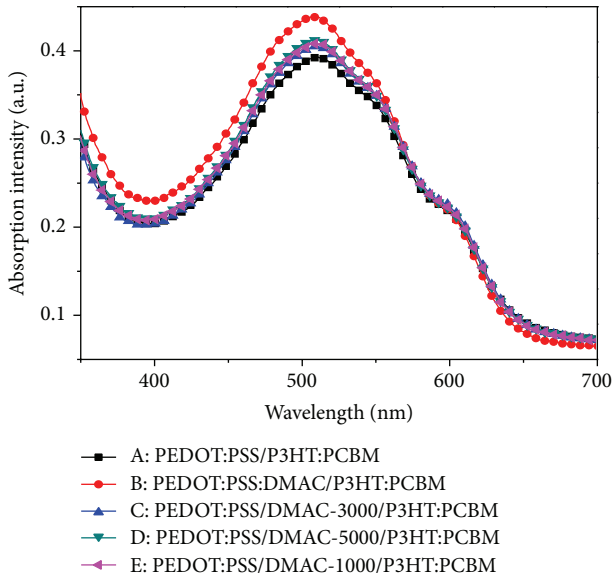

Figure 5: The absorption spectrum of PEDOT:PSS/P3HT:PCBM thin film. A: only PEDOT:PSS solution on ITO at the speed of 3000 rpm. B: the PEDOT:PSS and DMAC mixed in a ratio of 4 : 1 (v/v) at the speed of 3000 rpm. C, D, and E: the PEDOT:PSS buffer layer modified by DMAC at speed of 1000, 3000, and 5000 rpm.

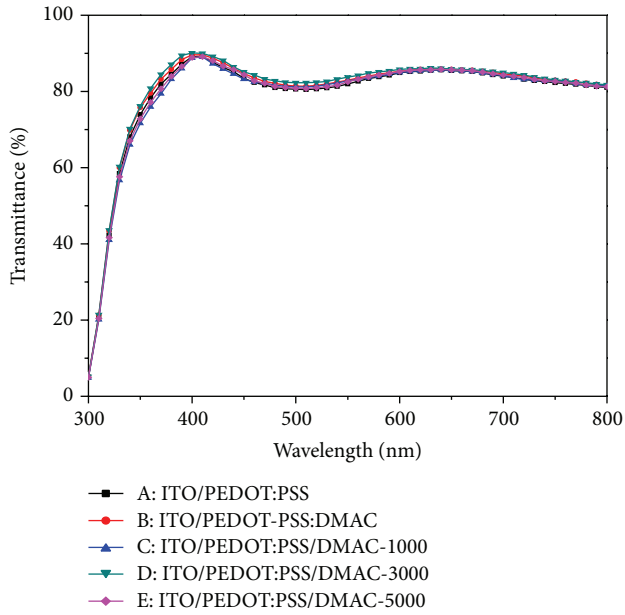

Figure 6: The transmission spectrum of ITO/PEDOT:PSS thin film. A: only PEDOT:PSS solution on ITO at the speed of 3000 rpm. B: the PEDOT:PSS and DMAC mixed in a ratio of 4 : 1 (v/v) at the speed of 3000 rpm. C, D, and E: the PEDOT:PSS buffer layer modified by DMAC at speed of 1000, 3000, and 5000 rpm.

conductivity also enhanced the film's charge transport capacity, enabling better charge extraction and collection as well as increasing short-circuit current and fill factor [21]. Figure 4 shows the dark J-V curves of various devices. At reverse bias, the current of DMAC-treated sample D rose more slowly with voltage, demonstrating that sample D had high shunt resistance. At forward bias, there were no obvious differences between DMAC-treated and untreated devices. The greater shunt resistance increased the FF, also increasing PCE.

From these results, we believe the inclusion of DMAC reduces the PEDOT:PSS energy barrier, which increased the conductivity of the active layer. This increase was most obvious when DMAC was spin-coated at 3000 rpm. Also, including DMAC changed the PEDOT:PSS chain morphology, increasing the roughness, which increased the contact area with the active layer and improved the generation and collection of extraction.

3.3. Absorption and Transmission of Visible and UV Light. Figure 5 shows the PEDOT:PSS/P3HT:PCBM thin film absorption spectrum with various buffer layers. The absorption of the DMAC-treated layer in 400–560 nm was better than that of the untreated layer. This improved the short-circuit current of the cell because it better absorbed ultraviolet and visible light. The enhanced absorption of the active layer increases the generation of excitons and short-circuit current. Device B had much better absorption than device D, but device B had lower short-circuit current density. Devices C, D, and E had essentially the same absorption, but their current densities differed much. This result shows that improving absorption is not the only way to improve

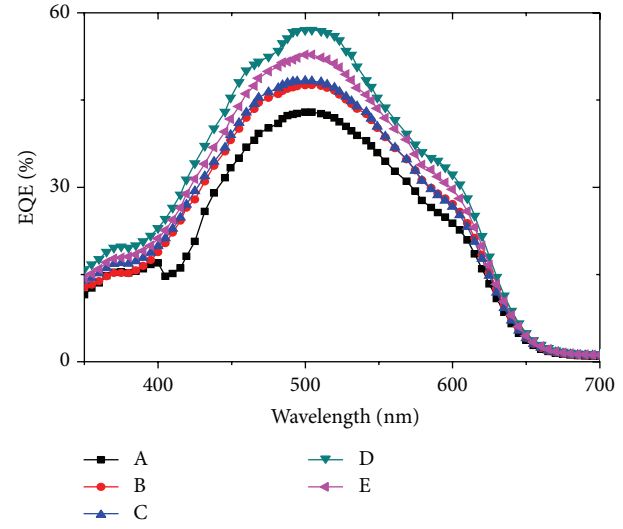

Figure 7: The external quantum efficiency spectra of five devices. A: only PEDOT:PSS solution on ITO at the speed of 3000 rpm. B: the PEDOT:PSS and DMAC mixed in a ratio of 4 : 1 (v/v) at the speed of 3000 rpm. C, D, and E: the PEDOT:PSS buffer layer modified by DMAC at speed of 1000, 3000, and 5000 rpm.

the short-circuit current density. Figure 6 shows the transmission spectrum of ITO/PEDOT:PSS thin film with various barrier layers. Compared with untreated ITO/PEDOT:PSS, the transmittance of the PEDOT:PSS treated by DMAC has little change. Although the PEDOT:PSS treated by DMCA has a lager transmittance, this has little effect on the conversion efficiency.

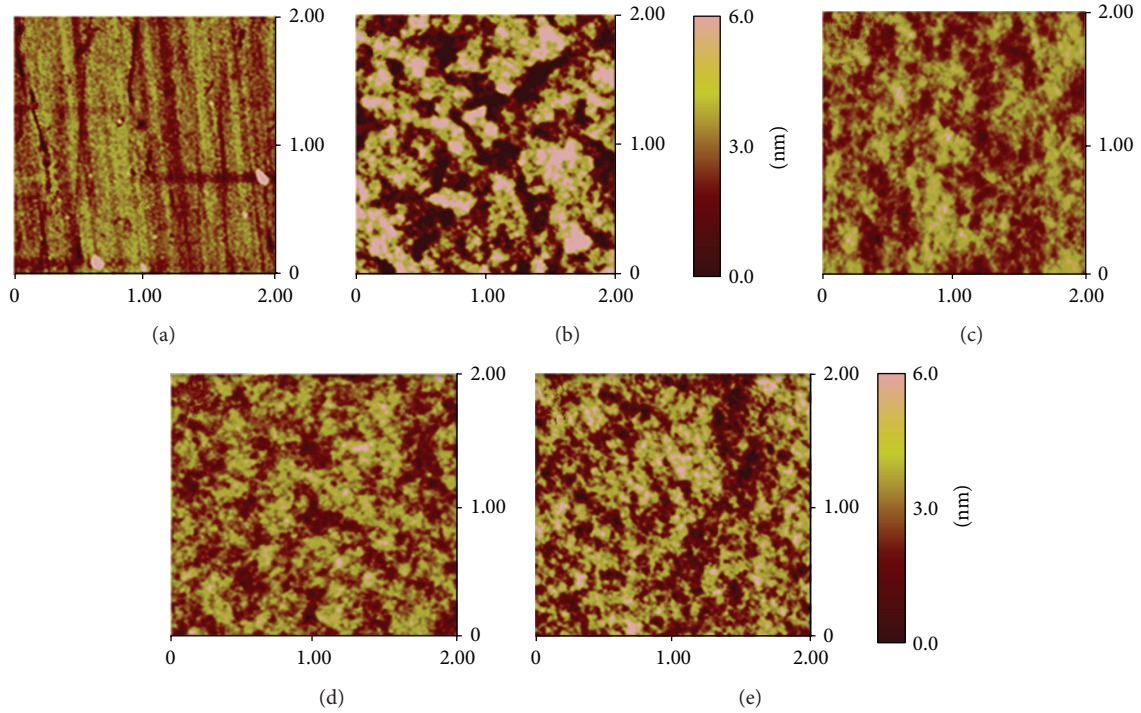

Figure 8: AFM images of different PEDOT:PSS devices. (a) Only PEDOT:PSS solution on ITO at the speed of 3000 rpm. (b) The PEDOT:PSS and DMAC mixed in a ratio of 4 : 1 (v/v) at the speed of 3000 rpm. (c), (d), and (e) The PEDOT:PSS buffer layer modified by DMAC at speeds (1000, 3000, and 5000 rpm).

3.4. External Quantum Efficiency. Figure 7 shows the external quantum efficiency spectra of devices. At wavelength of 300–900 nm, the DMAC-treated device spin-coated at 3000 rpm had much better efficiency at 500 nm than the untreated device. The external quantum effciency reached 57%. The short-circuit current density and conversion efficiency have great improvement.

3.5. Atomic Force Microscopy. To explain how DMAC affected cell performance, we used AFM to analyze the optimum shape of the anode buffer layer, as shown in Figure 8. Mixing PEDOT:PSS with DMAC leads to a nonuniform film, as shown in Figure 8(b), because DMAC and PEDOT:PSS do not dissolve into each other well. In contrast, spin-coating DMAC at a specific speed roughens the PEDOT:PSS film, increasing its contact area with the active layer. This increase improves hole transmission and reduces the recombination of holes and electrons. We hypothesize that treating the PEDOT:PSS film with DMAC may have changed the film's chain morphology, increasing the degree of phase separation and roughening the film [22]. The chain of PEDOT is transformed to linear or expansion crimp type structure from the curling type structure. As shown in Figure 8, the phase separation of PEDOT (bright area) is becoming bigger in the PEDOT:PSS that treated by DMAC and the conductivity of PEDOT:PSS improved. On the other hand, because spin-coating DMAC will remove the PSS from the top layer of PEDOT:PSS, this might have increased the electrical conductivity and film conductivity [23]. Because the active layer formed interpenetrating networks with the acceptor material, increasing the PEDOT:PSS roughness will connect these islands, forming an electronic transmission channel conducive to hole transmission [24].

4. Conclusions

Modifying the PEDOT:PSS anode buffer layer with DMAC improved the conversion efficiency of ITO/PEDOT:PSS/DMAC/P3HT:PCBM/LiF/Al organic solar cells. Characterizing the parameters of these cells, we found that DMAC-modified PEDOT:PSS improved the parallel resistance and conductivity of the devices. These changes improved the charge transport and collection in the cells, improving their conversion efficiency. These results suggest that modifying the anode buffer layer is one way to improve the photoelectric conversion efficiency.

Conflict of Interests

The authors declare that there is no conflict of interests regarding the publication of this paper.

Acknowledgments

The authors are grateful to the Natural Science Foundation of Hebei Province (F2012201089 and A2011201008), the Key Basic Research Project of Hebei Province (14964306D), and the key Project of Hebei Province Department of Education (ZH2011205 and ZD20131089) for financial support of this work.

References

[1] G. Yu, J. Gao, J. C. Hummelen, F. Wudl, and A. J. Heeger, "Polymer photovoltaic cells: enhanced efficiencies via a network of internal donor-acceptor heterojunctions," *Science*, vol. 270, no. 5243, pp. 1789–1791, 1995.

[2] B. C. Thompson and J. M. J. Frechet, "Organic photovoltaic polymer fullerene composite solar cells," *Angewandte Chemie—International Edition*, vol. 47, no. 1, pp. 58–57, 2008.

[3] G. Dennler, M. C. Scharber, and C. J. Brabec, "Polymer-fullerene bulk-heterojunction solar cells," *Advanced Materials*, vol. 21, no. 13, pp. 1323–1338, 2009.

[4] F. C. Krebs, J. Fyenbo, and M. Jørgensen, "Product integration of compact roll-to-roll processed polymer solar cell modules: Methods and manufacture using flexographic printing, slot-die coating and rotary screen printing," *Journal of Materials Chemistry*, vol. 20, no. 41, pp. 8994–9001, 2010.

[5] C. Deibel and V. Dyakonov, "Polymer-fullerene bulk heterojunction solar cells," *Reports on Progress in Physics*, vol. 73, no. 9, Article ID 096401, 2010.

[6] W. Cai, X. Gong, and Y. Cao, "Polymer solar cells: recent development and possible routes for improvement in the performance," *Solar Energy Materials and Solar Cells*, vol. 94, no. 2, pp. 114–127, 2010.

[7] Y. He and Y. Li, "Fullerene derivative acceptors for high performance polymer solar cells," *Physical Chemistry Chemical Physics*, vol. 13, no. 6, pp. 1970–1983, 2011.

[8] M. T. Dang, L. Hirsch, and G. Wantz, "P3HT:PCBM, best seller in polymer photovoltaic research," *Advanced Materials*, vol. 23, no. 31, pp. 3597–3602, 2011.

[9] R. C. Hiorns, R. De Bettignies, J. Leroy et al., "High molecular weights, polydispersities, and annealing temperatures in the optimization of bulk-heterojunction photovoltaic cells based on poly(3-hexylthiophene) or poly(3-butylthiophene)," *Advanced Functional Materials*, vol. 16, no. 17, pp. 2263–2273, 2006.

[10] H. Hoppe, M. Niggemann, C. Winder et al., "Nanoscale morphology of conjugated polymer/fullerene-based bulk-heterojunction solar cells," *Advanced Functional Materials*, vol. 14, no. 10, pp. 1005–1011, 2004.

[11] W. Ma, C. Yang, X. Gong, K. Lee, and A. J. Heeger, "Thermally stable, efficient polymer solar cells with nanoscale control of the interpenetrating network morphology," *Advanced Functional Materials*, vol. 15, no. 10, pp. 1617–1622, 2005.

[12] L. Y. Yang, H. Xu, H. Tian et al., "Effect of cathode buffer layer on the stability of polymer bulk heterojunction solar cells," *Solar Energy Materials and Solar Cells*, vol. 33, pp. 233–237, 2012.

[13] Y. Wang, L. Yang, C. Yao, W. Qin, S. Yin, and F. Zhang, "Enhanced performance and stability in polymer photovoltaic cells using lithium benzoate as cathode interfacial layer," *Solar Energy Materials and Solar Cells*, vol. 95, no. 4, pp. 1243–1247, 2011.

[14] J. Jung, D. Kim, S. S. Won et al., "The effect of molybdenum oxide interlayer on organic photovoltaic cells," *Journal of Applied Physics*, vol. 95, no. 9, Article ID 093304, 3 pages, 2010.

[15] J. Subbiah, D. Y. Kim, M. Hartel, and F. So, "MoO_3/poly(9,9-dioctylfluorene-co-N-[4-(3-methylpropyl)]-diphenylamine) double-interlayer effect on polymer solar cells," *Applied Physics Letters*, vol. 96, no. 6, Article ID 063303, 2010.

[16] P. Peumans and S. R. Forrest, "Very-high-efficiency double-heterostructure copper phthalocyanine/C60 photovoltaic cells," *Applied Physics Letters*, vol. 79, no. 1, pp. 126–128, 2001.

[17] S. H. Eom, S. Senthilarasu, P. Uthirakumar et al., "Polymer solar cells based on inkjet-printed PEDOT:PSS layer," *Organic Electronics: Physics, Materials, Applications*, vol. 10, no. 3, pp. 536–542, 2009.

[18] S. I. Na, S. S. Kim, J. Jo, and D. Y. Kim, "Efficient and flexible ITO-free organic solar cells using highly conductive polymer anodes," *Advanced Materials*, vol. 20, no. 21, pp. 4061–4067, 2008.

[19] F. C. Krebs, T. Tromholt, and M. Jørgensen, "Upscaling of polymer solar cell fabrication using full roll-to-roll processing," *Nanoscale*, vol. 2, no. 6, pp. 873–886, 2010.

[20] A. M. Nardes, M. Kemerink, R. A. J. Janssen et al., "Microscopic understanding of the anisotropic conductivity of PEDOT:PSS thin films," *Advanced Materials*, vol. 19, no. 9, pp. 1196–1200, 2007.

[21] F. C. Krebs, "Fabrication and processing of polymer solar cells: a review of printing and coating techniques," *Solar Energy Materials and Solar Cells*, vol. 93, no. 4, pp. 394–412, 2009.

[22] M. D. Perez, C. Borek, S. R. Forrest, and M. E. Thompson, "Molecular and morphological influences on the open circuit voltages of organic photovoltaic devices," *Journal of the American Chemical Society*, vol. 131, no. 26, pp. 9281–9286, 2009.

[23] D. Gupta, M. Bag, and K. S. Narayan, "Correlating reduced fill factor in polymer solar cells to contact effects," *Applied Physics Letters*, vol. 92, no. 9, Article ID 093301, 2008.

[24] Y. Xia and J. Ouyang, "PEDOT:PSS films with significantly enhanced conductivities induced by preferential solvation with cosolvents and their application in polymer photovoltaic cells," *Journal of Materials Chemistry*, vol. 21, no. 13, pp. 4927–4936, 2011.